Long-range transmission at low elevations over the ocean

A.N. de Jong, G. de Leeuw, P.J. Fritz, M.M. Moerman
TNO Physics and Electronics Laboratory
PO Box 96864
2509 JG The Hague
The Netherlands

1. SUMMARY

Results are presented from infrared transmission measurements over long ranges at low elevation in coastal waters. This work was part of the EOPACE programme, conducted at two locations along the US West Coast. In this programme data were collected for validation of atmospheric models, used to predict IR sensor performances.
Details are given on the transmissometer set-up and measurement methodology. The data concern midwave (3-5μm) and longwave (8-12 μm) measurements, taken over the Monterey Bay (22 km) and San Diego Bay (15 km) in various periods of the year (March, April, August and November).
The results are compared with model predictions, including molecular extinction, aerosol scattering and refraction effects. The first two effects have been determined carefully and could be quantified to a certain extent with the help of simultaneously collected meteorological data. The refraction effects are of a more complicated nature due to the complex temperature profile structure over water, which is difficult to measure.

2. INTRODUCTION

The effects of water vapour and aerosols on infrared (IR) propagation through the atmosphere are well known and described in the literature [1]. As a result of the extinction due to these effects, the detection range of IR sensors is limited. For a point target, this detection range (R_d) is directly related to the transmission by the following formula:

$$R_d = \sqrt{\frac{\Delta W * \tau(R_d)}{NEI * (S/N)_t}} \qquad (1)$$

In this formula ΔW is the target contrast (W/sr), $\tau(R_d)$ the atmospheric transmission in the respective band over the range R_d, NEI the sensor's Noise Equivalent Irrandiance (W/m^2) and $(S/N)_t$ the threshold signal to noise ratio.
For Infrared Search and Track sensors (IRST) interesting ranges are between 10 and 30 km, when detection of incoming missiles is envisaged. For these ranges the effect of water vapour and aerosols on transmission based upon Lowtran 7 predictions in the midwave and longwave IR is illustrated in figures 1, 2 and 3.
The effect of water vapour is shown in figure 1, where the transmission appears to decrease strongly with absolute humidity, as generally known the longwave IR much more rapidly than the midwave.

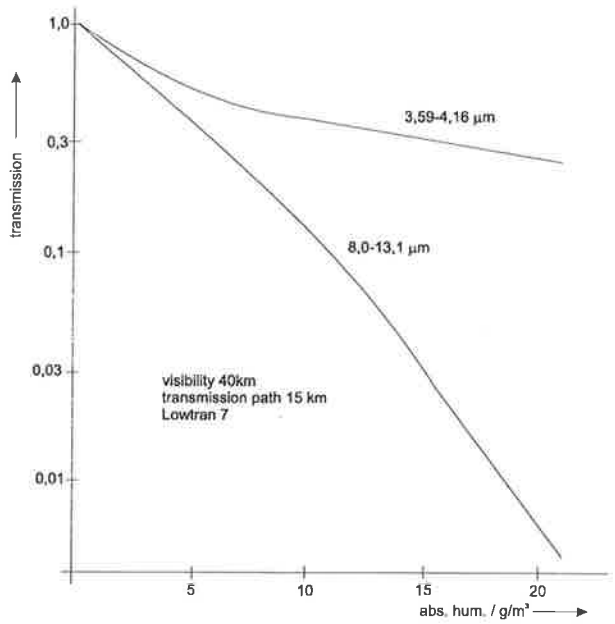

Fig. 1: Midwave and longwave IR transmission versus absolute humidity.

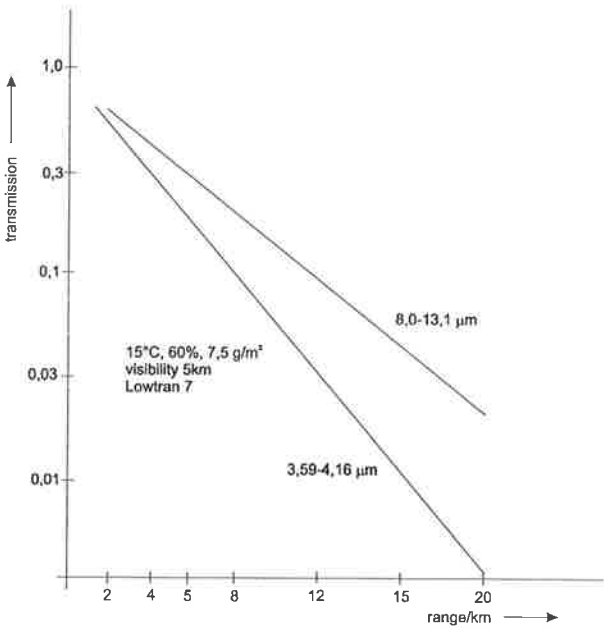

Fig. 2: Midwave and longwave IR transmission versus range.

Paper presented at the RTO SET Symposium on "E-O Propagation, Signature and System Performance Under Adverse Meteorological Conditions Considering Out-of-Area Operations", held at the Italian Air Force Academy, Naples, Italy, 16-19 March 1998, and published in RTO MP-1.

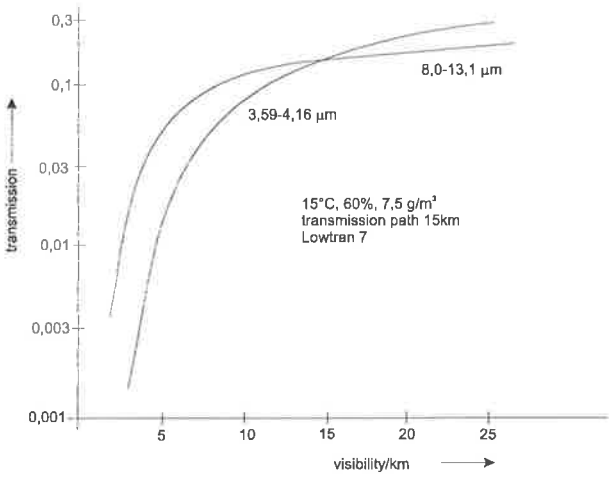

Fig. 3: Midwave and longwave IR transmission versus visibility.

The calculations were made for rather clear bands without CO_2 absorption and a visibility of 40 km. For ranges of about 15 km, we can write for the transmission values τ_m and τ_l for midwave and longwave as function of range R respectively

$$\tau_m = \exp(-\sigma_m R) \qquad \tau_l = \exp(-\sigma_l R) \qquad (2)$$

where τ_m and τ_l are the midwave respectively longwave extinction coefficients, approximately related to the absolute humidity h_a by

$$\tau_m = 0.0054\ h_a \qquad \tau_l = 0.0156\ h_a \qquad (3)$$

For $h_a = 15$ g/m^3 we find $\tau_m = 0.08$ km^{-1} and $\tau_l = 0.23$ km^{-1}.
Figure 2 shows the transmission as function of R, for a visibility of 5 km. The midwave transmission decreases more rapidly than the longwave IR transmission.
For an absolute humidity of 7.5 g/m^3, resulting in τ_m and τ_l values of about 0.04 km^{-1} resp 0.12 km^{-1} for water vapour, the total, combined extinction coefficients for a visibility of 5 km due to water vapour and aerosols are 0.28 km^{-1} resp 0.19 km^{-1}. The contributions of aerosols to these values are 0.24 km^{-1} resp 0.07 km^{-1} for midwave and longwave IR.
Figure 3 shows an example of the variation of the transmission over a 15 km path with the visibility. For visibilities greater than 12 km, the effect of the visibility becomes almost negligible.
As an example we demonstrate the transmission effect on the detection range by substituting in formula (1) for NEI the midwave and longwave values of 10^{-10} W/m^3 resp 4.10^{-10}W/m^2, for ΔW: 0.2 resp 1 W/ster (a low observable missile) and $(S/N)_t = 5$, an atmosphere of 15 g/m^3 and visibility of 40 km. R_d is found to be 12,2 resp 8,4 km for the midwave resp longwave sensor.
So far theory and measurements are rather well in agreement for open ocean conditions with similar air and sea temperatures which are known along the path, known aerosol size distribution, and along paths that are not close to the sea surface.
In a coastal environment however, with high probability of inhomogeneities along the path and targets skimming the ocean at low altitude (for example 3 m), detection ranges are much more difficult to predict. Both the MAPTIP trials [2] and other propagation measurements over long ranges over the North Sea [3] have shown strong anomalies in propagation effects.
In order to further investigate these anomalies, TNO-FEL, sponsored by the Netherlands Ministry of Defence and ONR, decided to participate in the EOPACE campaign (Electro Optical Propagation Assessment in Coastal Environment) organized at two locations along the US West Coast, well known for the atmospheric imhomogeneities, provided by generally cold water close to a desert-like land environment. Preliminary measurements by Bull [4] clearly showed the anomalies due to low level and along path gradients in temperature, humidity and particle size distribution. Unfortunately very few support data (e.g. aerosol and meteorological data) were taken during Bull's measurements. During the EOPACE campaign this was done much more carefully [5]. This provided a strong basis and data set for further validation of low level propagation models. The input from TNO-FEL in this programme consisted of transmissometry and collection of aerosol size distributions and meteorological data. Preliminary results on the transmissometry have been reported in [6] for the first phase of the project: the measurements in Monterey and San Diego in March and April 1996. Preliminary results on the second phase of the project, concerning transmission measurements in San Diego in November 1996 and August 1997 are reported in [7].
This paper contains an overview of the results of the transmissometry, the lessons learned and recommendations for the work to be carried out in the future.

3. DESCRIPTION OF SET-UP

Two locations have been chosen for the transmissometry: Monterey Bay with a 22 km path between Moss Landing Pier and Monterey Plaza hotel and San Diego Bay with a 15 km path between Imperial Beach Pier and the Naval Sub Base BOQ. Both paths are schematically shown in figures 4 and 5.

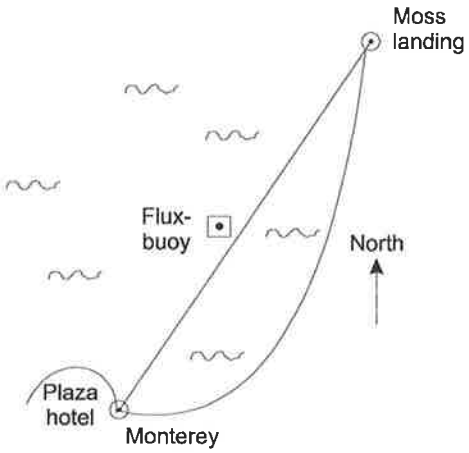

Fig. 4: Measurement path in Monterey.

The ranges are of operational interest concerning the detection of targets at an altitude of 3 m with a sensor at an altitude of 15 m. This causes the target to pop up over the horizon at a range of 19.4 km. For reasons of safety for the equipment we

mounted the transmissometer source at an altitude of 10 m above mean water level at Moss Landing and at 9 m altitude at Imperial Beach. The receivers were mounted at altitudes of 16.5 m resp 5.4 m in Monterey resp San Diego.

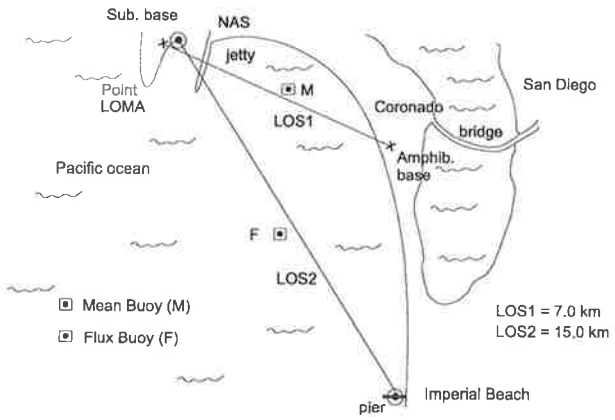

Fig. 5: Measurement path in San Diego.

Technical details on the transmissometer are presented in table 1. The transmissometer is basically similar to the one, used in earlier measurements over 18 km in the North Sea environment [8]. The transmitter and the receiver have identical Newtonian mirror optics with 230 cm^2 effective entrance pupil area.

Table 1: Technical parameters of TNO-FEL transmissometer.

Parameter	Value
Source collimator diameter	20 cm
Source focal length	40 cm
Source temperature	900 K phase 1; 1100 K phase 2
Beam divergence	10 mr phase 1; 6.25 mr phase 2
Chopping frequency	820 Hz
Useful source area	230 cm^2
Receiver collimator diameter	20 cm
Receiver focal length	40 cm
Midwave detector type	HgCdTe phase 1; InSb phase 2
Midwave detector size	2x2 mm phase 1; 2 mm round phase 2
Midwave spectral bands	3.7-5.7 µm phase 1; 3.60-4.04 µm phase 2, Nov. 3.59-4.16 µm phase 2 Aug.
Longwave detector size	2x2 mm
Longwave spectral band	8.0-13.1 µm

A reference signal was transmitted by means of a radio link and used for synchronous detection of the 820 Hz modulated signal. The time constant was normally set at 3 sec and the signal was sampled with a frequency of 1Hz. The signal to noise ratio for the 22 km range was about 600 resp 150 for the midwave resp longwave band for 100% transmission condition in phase 1 (March/April '96).
By averaging the signals over a period of 1 minute, the signal to noise ratio's improve a factor of 4.5. This means that a 1% longwave transmission level can be measured with an accuracy of 15%, which is acceptable (for the 1 minute integration time). The midwave transmission level is measured with a 4 times better accuracy.

It is noted that the set-up was slightly modified and improved during the campaigns. From phases 1 to 2, a new source with higher temperature was mounted to provide a higher signal to noise ratio. Also the HgCdTe midwave detector was replaced by an InSb one because of better homogeneity of the responsivity over the detector area.
The spectral bandfilter for the midwave band was changed to have better band correspondence with the SPAWAR transmissometer, simultaneously operating over a 7 km path in San Diego (see figure 5, [9]).
In the first three campaigns the transmissometer was operated with a midwave or longwave detector. In the fourth campaign 3 transmissometers were operated simultaneously; one midwave band in room 246 of the BOQ and two in room 146. The 2 lower receivers (midwave + longwave) in room 146 were at an altitude of 6.4 m above mean sea level; the receiver in room 246 at 9.4 m above mean sea level. This set-up provided an opportunity to investigate the dependence of transmission on height above the water.
The additional equipment, used in the various experiments consisted of:

- particle size distribution measurements (Knollenberg type) at Moss Landing Pier and Imperial Beach Pier
- meteorological equipment
- high resolution midwave imager in Monterey and San Diego during the first phase
- high resolution near IR camera
- near IR radiometer and 1000 Hz source for scintillation measurements in phase 1 and August '97 phase 2
- midwave camera for point source measurements in August '97, phase 2.

Results on the scintillation measurements have been reported in [10]. The near IR camera's were used to visually inspect the atmospheric behaviour. For this purpose, an alignment source was mounted near the transmitters. The transmitters in turn were aligned with a similar alignment source at the receiver side.

4. CALIBRATION, SIGNAL HANDLING

As signal(s) we will consider here the signal from the Lock-In amplifier, which provides the time averaged (3 sec) RMS value of the 820 Hz signal, coming from the transmitter. As transmission along the path we measure by definition

$$\tau = \frac{\textit{signal with atmosphere}}{\textit{signal without atmosphere}} = \frac{\int_{\lambda_1}^{\lambda_2} e(\lambda)\tau(\lambda)\rho(\lambda)d\lambda}{\int_{\lambda_1}^{\lambda_2} e(\lambda)\rho(\lambda)d\lambda} \qquad (2)$$

in which $e(\lambda)$ is the source spectral emission, $\rho(\lambda)$ the receiver spectral response and $\tau(\lambda)$ the atmospheric spectral transmission.
It is important to note that all power received in the full instantaneous field of view, is taken into account. This means that possible contributions in the signal due to forward scattering by aerosols and refraction effects are included.

The determination of the 100% value from formula (2) is difficult because we cannot easily create a longwave vacuum path. In the meantime a zero range calibration (to make $\tau(\lambda)=1$) causes a lot of optical problems, because it is questionable whether the transmitter and receiver can be aligned in such a way that no signal is lost by obscuration. Therefore we calibrated our transmissometer by measurement of the signals on two clear days over a path of 800 m and 2500 m near our laboratory in The Hague. For the atmospheric conditions at these days both integrals in formula (2) were calculated using Lowtran 7.
The signals for the 800 m and 2500 m ranges corresponded within a few percent, which gave us confidence in the method. Denoting the 5μm and 10 μm signal over 2500 m by $s_{2.5}(5)$ resp $s_{2.5}(10)$ and the τ values $\tau_{2.5}(5)$ resp $\tau_{2.5}(10)$, we find for the transmission over the 22 km range:

$$\tau_{22}(5) = \frac{s_{22}(5)}{s_{2.5}(5)} \cdot \frac{22^2}{2.5^2} \tau_{2.5}(5) \quad resp$$
$$\tau_{22}(10) = \frac{s_{22}(10)}{s_{2.5}(10)} \cdot \frac{22^2}{2.5^2} \tau_{2.5}(10) \qquad (3)$$

where $s_{22}(5)$ resp $s_{22}(10)$ are the midwave resp longwave longrange (22 km) signals. For the 15 km range we take 15 instead of 22 in formula (3).
Before the calibration over 800 m resp 2500 m, we performed a number of laboratory measurements to check the components of the system:

- measurement of detector responsivities (D*)
- measurement of spectral transmission of filters
- compare the 900 K source with a calibrated blackbody and measure its real temperature
- measure the source radiant intensity with detector and filter without optics
- measure the homogeneity of the emission/sensitivity over the pupil, test of optics transmittance/mirror reflectance
- test of the Lock-In amplifier, measure the noise histogram of the output signals
- test the homogeneity of the detector response over its surface with the 800 m outside experiment. Here we found the problem with the HgCdTe detector mentioned above.

Because in the first three campaigns we could measure with only one detector at a time (midwave or longwave), we frequently had to change the gain (and the phase!) of the Lock-In amplifier. Most of the times one detector was used in the receiver during between 3 and 6 hours.
In the fourth campaign (San Diego, August '97), the 'classic' receiver (room 246) was provided with a midwave detector, whereas the two receivers in room 146 had a midwave and longwave detector. The diameter resp focal length of these two receivers were 20 cm resp 50 cm. The 3 Lock-In amplifiers each had a different signal handling, which has been taken into account.

5. RESULTS

The general first impression of the results of the 4 transmission campaigns along the US West Coast is one of great variability. The expected atmospheric inhomogeneities did occur, as well along the path as in altitude. Rapid variations of these conditions in time occurred and it became clear that transmittance values are very much dependent upon altitude of sources and receivers.
A visual impression of image distortion due to refraction is shown in figures 6 and 7, where the image of a point source is shown, as transmitted through the atmosphere over Monterey Bay. Striking is the fact that in figure 6, the source is just above an inversion layer, but in figure 7 just in the middle. The result is a vertically elongated line source. The pictures were taken in daytime.
Figure 8 shows a normal, frequently occurring mirage in San Diego. The mirage occurs when a cool air layer strikes over water. Sometimes the mirages occur in the middle of the night, sometimes in the early morning. Mostly these conditions lead to increased transmission values, as the intensity of both mirage components are similar and both fall on the detector. Figures 9-12 show results of transmission measurements in the four campaigns.
'Normal' transmission values for the 22 km range in Monterey for midwave (3.7-5.7 μm) and longwave (15°C, 70%) are about 7% resp 4%. Evident are the large increases by more than a factor 5 due to refraction effects, as visually illustrated in figure 7. The magnitude of this factor is difficult to predict when the temperature profile (at various locations) along the transmission path is not accurately known. It is clear that the knowledge of just one temperature at one altitude is insufficient.
Many authors have presented models to predict this refraction effect. Forand [11] and Dion [12] have integrated the effect in a complete atmospheric propagation model for marine boundary layers (IRBLEM). Church [13] presents the refraction effect as part of the IRST model IR Tool, developed by Areté associates. Besides these efforts, many authors have presented work, including attempts to retrieve the layering structure from sunset mirages [14, 15, 16, 17]. Unfortunately sunset and sunrise occur only once a day, so other methods are required to measure the temperature profile. Our own observation during EOPACE is that often strong gradients occur over a very short distance, so that the mirage seems to be a real reflection to a 'hard' surface.
An essential point is, that the transmissometer-receiver has such a large field of view (5 mrad) that all refraction effects are integrated. This means that the measured transmission value is of no direct significance for IRST's with an instantaneous field of view of circa 0.2 mrad. We can therefore not simply use for $\tau(R_0)$ in formula (1) the measured value of τ.
In this case, transmission as measured with a calibrated imager such as done in the LAPTEX experiments at Crete [18] is preferable and this value can directly be inserted in formula (1). The disadvantage is the increased uncertainty due to scintillation at long range.
During the campaign in Monterey some conditions occurred with fog and rain, most of the time only present along part of the path. The mirage conditions occurred frequently, nearly every day.

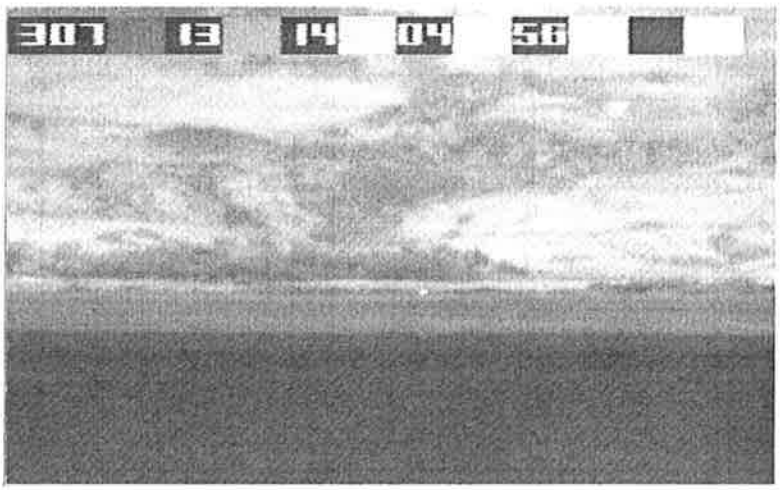

Fig. 6: Near IR picture of point source over Monterey Bay just above 'inversion' layer; 22 km; 7 March '96.

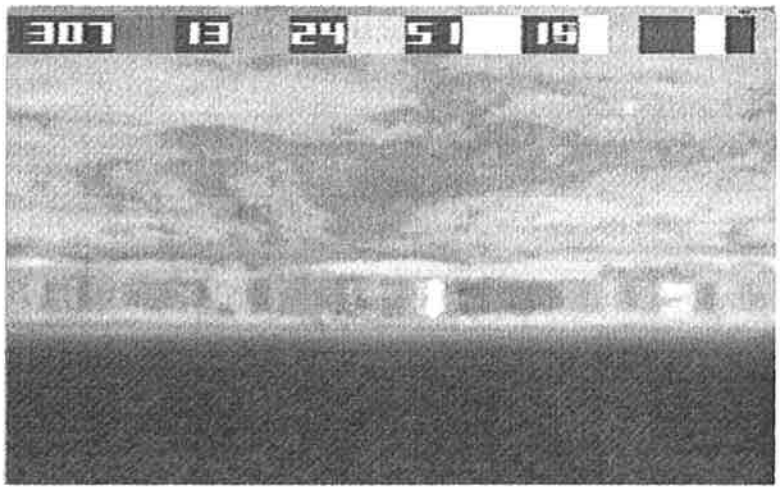

Fig. 7: Same picture as figure 6, 10 minutes later; point source in layer; strong refraction effect.

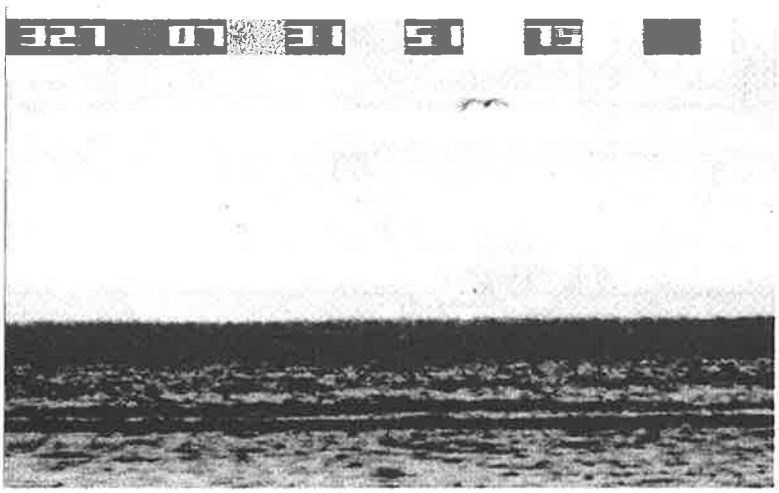

Fig. 8: Mirage condition 27 March '96 over San Diego Bay.

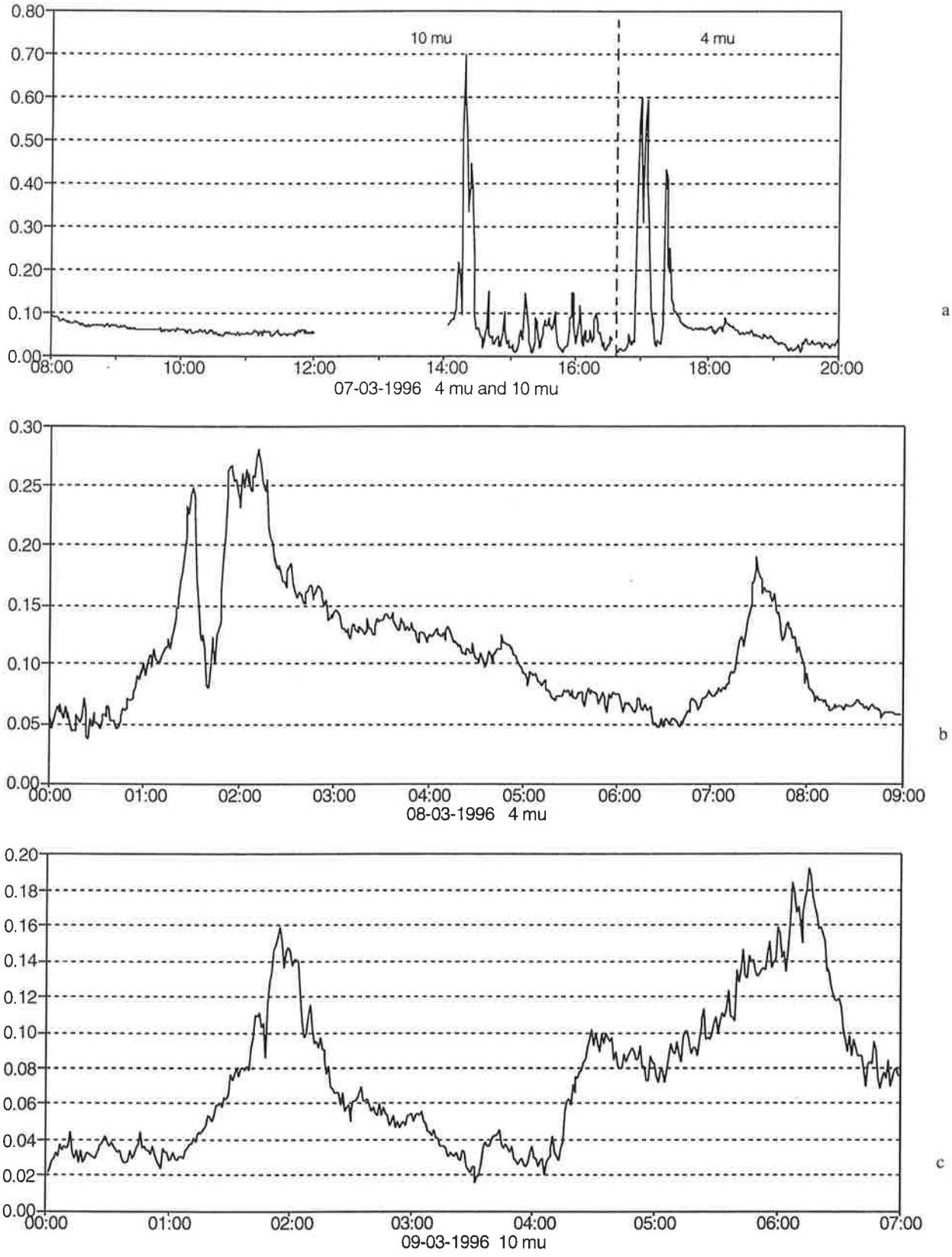

Fig. 9: Results of transmission measurements in Monterey, March '96.

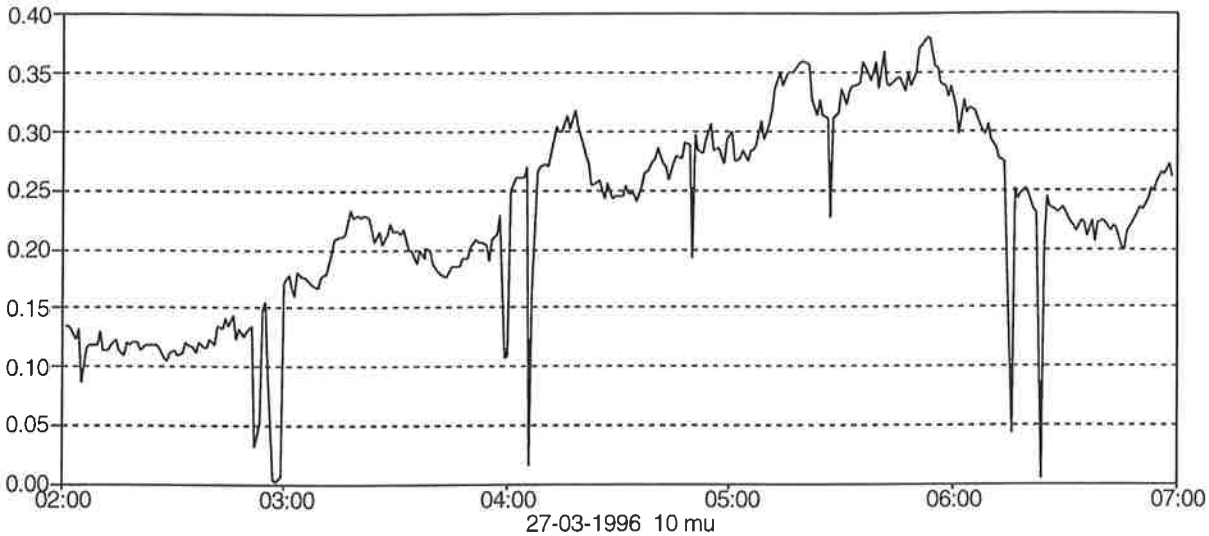

a

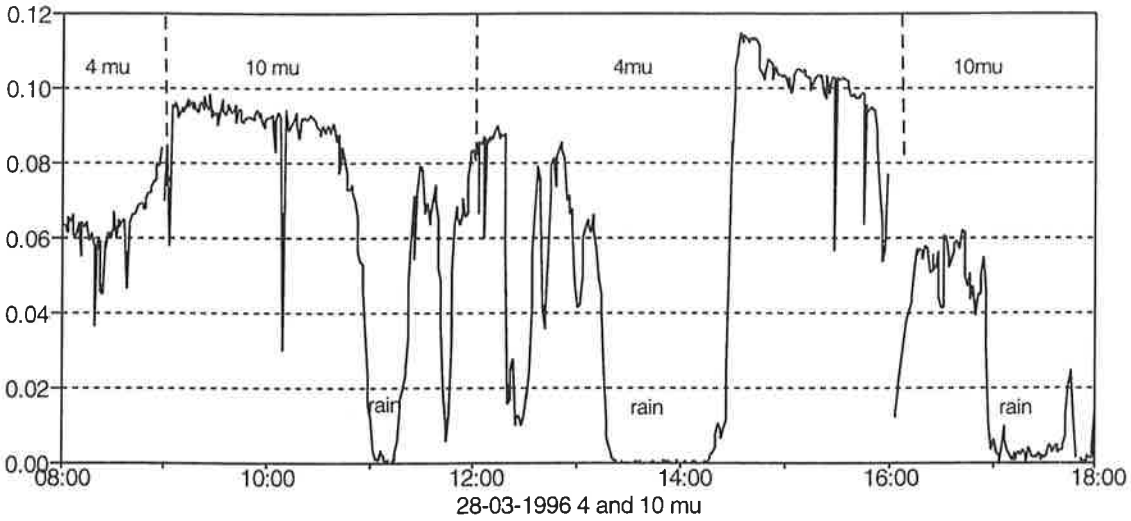

b

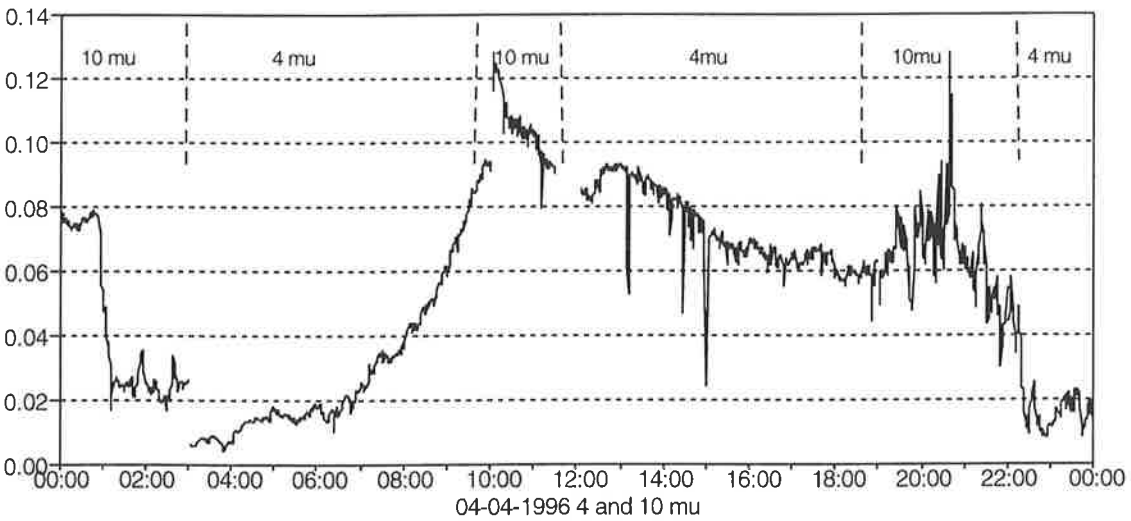

c

Fig. 10: Results of transmission measurements in San Diego, March/April '96.

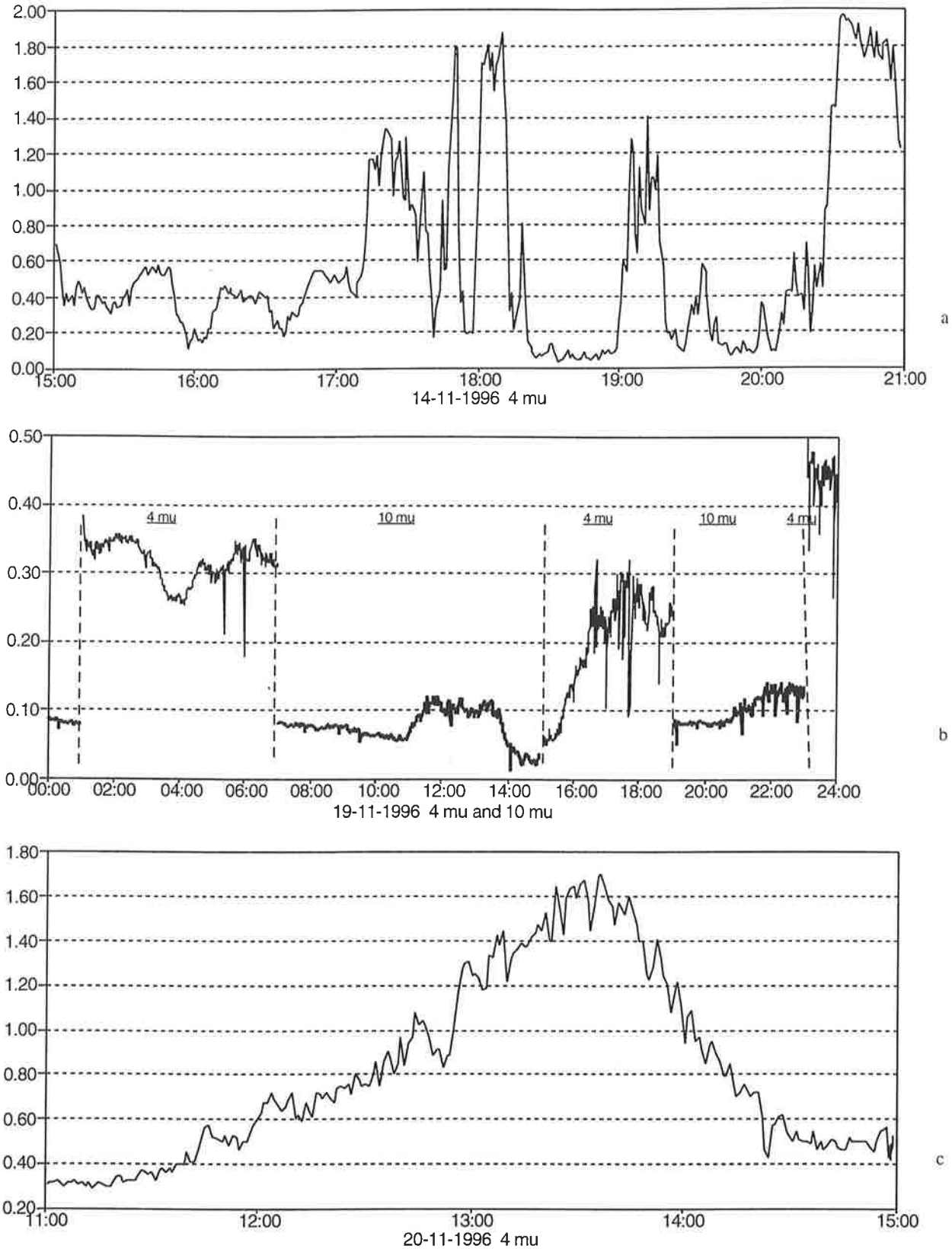

Fig. 11: Results of transmission measurements in San Diego, November '96.

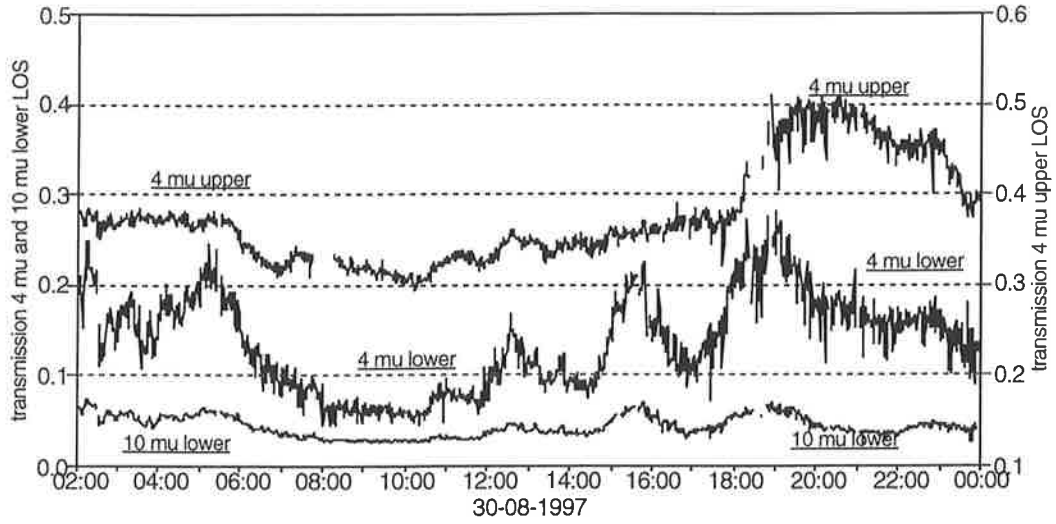

a

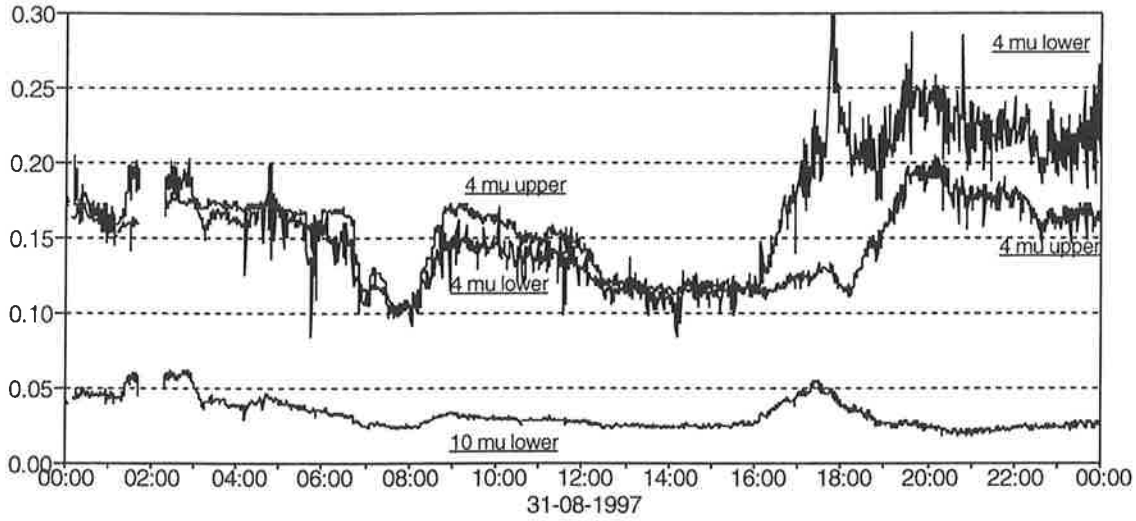

b

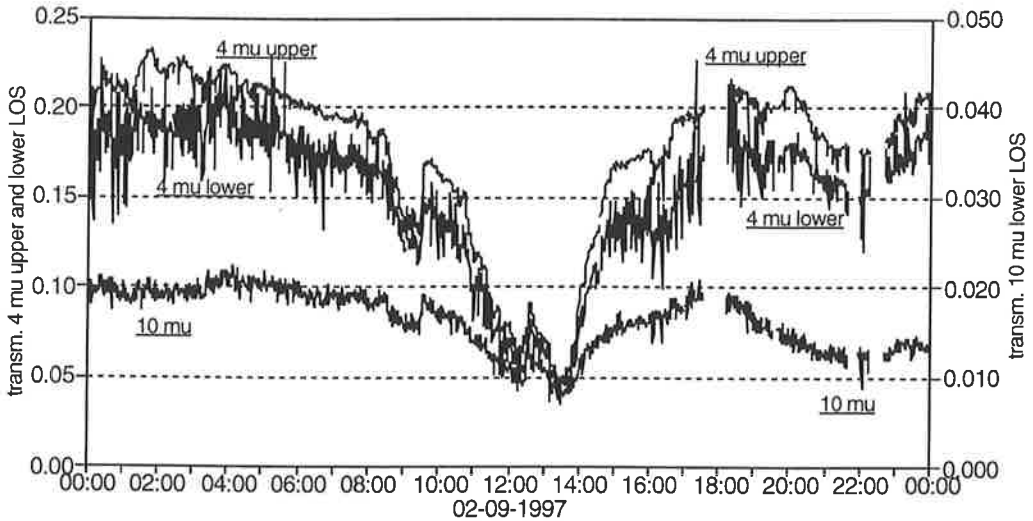

c

Fig. 12: Results of transmission measurements in San Diego, August/September '97.

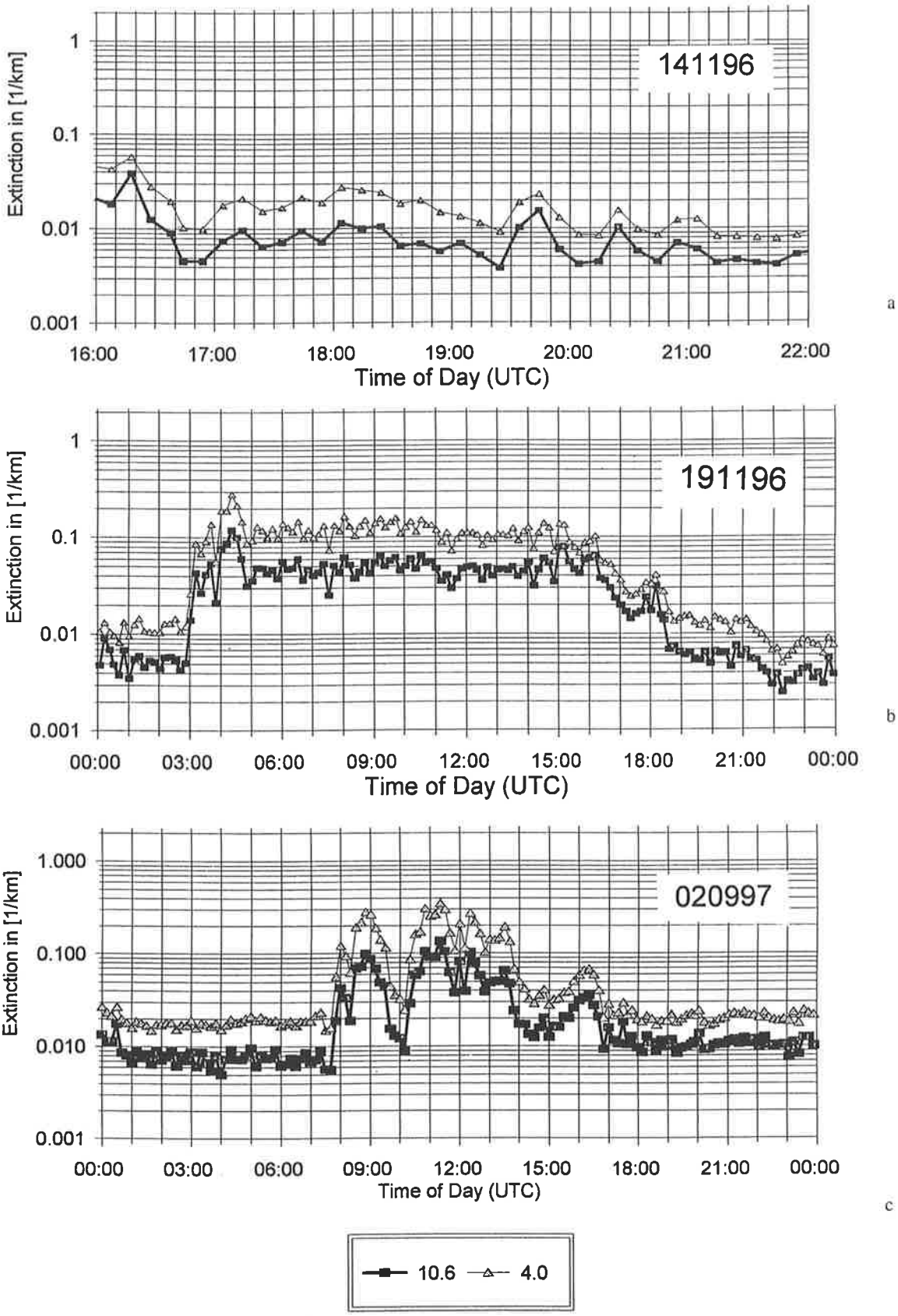

Fig. 13: Results of aerosol measurements in November '96 and August/September '97.

Results of the second campaign in San Diego, in March/ April '96, are shown in figure 10. Again the subrefractive conditions occurred, resulting in excessive transmission values. While 'normal' transmission values for the local meteorological conditions are of the order of 10-15% for longwave, we observe a sudden increase to nearly 40% on the 27th of March near 6 a.m.

This phenomenon is illustrated by the image of the mirage in figure 8. The lower point source is the mirage, in this case just before being hidden behind the horizon. The angular separation between the real and mirage source is 0.87 mrad, which is typical for the 15 km range over the San Diego Bay. A similar separation was reproduced in many other occasions. Striking is the sharpness of the mirage point source, which can only be explained if the refraction effect is taking place in a thin layer of cold air, behaving as a reflector. The midwave transmission values are similar to those in the longwave band (≈10%). We have to realize here, that the 3.7-5.7 μm band contains a lot of water vapour absorption lines, causing saturation in the 4.8-5.7 μm wavelength region. In addition the CO_2 band at 4.25 μm also causes saturation. Taking into account only the spectral band 3.59-4.16 μm (see figure 1), the transmission value would be close to 30%, for a visibility of 25 km.

Figure 10 shows also some periods with zero transmission due to rain somewhere in the path (figure 10.b). Figure 10.c shows a gradual increase in midwave transmission between 3 and 10 a.m. accompanied by a gradual change of visibility. The particle size distributions as measured at the Imperial Beach Pier, could not explain this behaviour quantitatively; apparently the aerosol was not homogeneously distributed along the path.

Figure 11 shows November '96 transmission data with the new midwave detector and filter. The time is given in GMT in these plots, which is identical to local time + 8 hours in winter. On average, the midwave transmission value is 35% and for longwave again around 10%. These values correspond well with the predictions from figures 1 and 3. Interesting is the result of the aerosol measurements; as shown in figure 13 the midwave/longwave extinction coefficients are about 0.02/0.01 km^{-1} respectively, which for a range of 15 km corresponds to a transmission due only to aerosols of 0.75 resp 0.86.

Interesting again is the refraction effect in the morning on the 14th and during the night of the 20th. The midwave transmission went up to values of 200%! Similar to figure 9.a, the transmission values were fluctuating strongly with time. One factor could be the tide, which changes the altitude of the beam with respect to the air layers.

Interesting also is the aerosol effect on the 19th. The aerosol measurements (figure 13.b) show a midwave extinction coefficient of 0.1 km^{-1} corresponding to an aerosol transmission of 0.22 over the 15 km path. The transmission data show transmission values (including molecular extinction) of 0.30 and more until 7 a.m. Apparently the particle size measurements were not representative for those along the whole transmission path, the location being higher at Imperial Beach than at other places. Another effect might be due to particles, produced in the surf zone or particles, produced locally ashore. The wind direction was indeed between East to the North.

Around 13.30 the longwave transmission rapidly decreased to a few percent, which similar to the midwave transmission decreased to about 7%. After that period we observe a rapid increase of transmission to 25% midwave. Since no changes were observed in the extinction coefficients (figure 9.b) while during a short period around 14.00 the wind direction changed to North for about an hour, the observed variations must be due to local variation of aerosol and/or meteorological properties along the transmission path.

Refraction effects were observed on the 20th around 13.30 GMT (= 05.30 local time). The increase was about a factor 5.

Figure 12 shows results of the 4th campaign in August/September '97 in San Diego. Each of the figures shows 3 plots: one of the upper level midwave channel and two of the lower level midwave and longwave channels. Figure 12.a shows clearly that the lower midwave channel transmission between 01.00 and 06.00 GMT (evening of 29th of August) has a transmission of about 30%, while the higher level has a transmission of 20%. The difference is probably due to sub-refraction for the lower level transmissometer. Later on that day (between 20.00 and 22.00) the midwave transmission at the higher elevation rises towards the midwave at the lower level, while the longwave level drops. This is probably due to a thin haze layer over the water surface.

The average values of the transmission for this period were below those of previous campaigns. We measured about 20% for midwave and 4% for longwave. The main reason for this was the higher absolute humidity. With an air temperature of 20°C and a relative humidity of 80%, the absolute humidity is 14 g/m^3.

From figure 1, midwave resp longwave transmissions taking into account only molecular absorption are 30% resp 4.6%. Looking more closely to the aerosol extinction, midwave resp longwave extinction coefficients are on the order of 0.03 resp 0.02, corresponding to aerosol transmissions of 0.64 resp 0.74. With these values, the total predicted transmission becomes 19% resp 3.4%, which corresponds well with the measured data.

Figure 12.b shows similar effects as figure 12.a. The higher elevation transmission is significantly and most of the time larger than the lower level transmission except for a short time around 17.00, when due to refraction the lower level transmissions increase by about a factor 2.

Figure 12.c shows the transmission plot for 2 September. The only effect of significance is a strong reduction in transmission around 12.00 GMT (4 a.m.) due to aerosols. In figure 13.c,a strong increase in extinction occurs from 08.00 GMT which explains the observed decrease in transmission. The wind direction was observed to change from East to North around 11.00 GMT. Apparently these Northerly winds carried the aerosols causing the drop in transmission. The extinction coefficient of 0.2 however predicts an aerosol transmission of 5% which is a much stronger effect than measured from the transmissometry. It is apparent that the midwave transmissions (both upper and lower level) are affected about 2× stronger than the longwave transmission.

6. CONCLUSIONS

The four transmission measurement campaigns, carried out in the framework of EOPACE along the US West Coast, have provided an interesting data set for investigation of the variability of atmospheric transmission behaviour due to instabilities and inhomogeneities in temperatures and their profiles, humidity and aerosol size distribution. For normal conditions Lowtran 7 predicts the transmission reasonably well. Refraction effects cause a strong deviation; one reason is that during transmission measurements the detector receives the sum of all mirage intensities in its field of view, being considerably larger than in operational IR sensors.

It is noted that the measured transmission values should not be used directly in IRST range performance formula due to the difference in Instantaneous Field of View of the transmissometer receiver and the IRST sensor.

It has been found that aerosol and meteorological measurements carried out only at the end of the measurement path, does not provide sufficient data for use as input for the propagation prediction models used to explain the observed transmission phenomena. Even the buoy in the middle and the sensor package on the boat do give a too local, insufficient set of input data. To fully predict the refraction effect, a very detailed profile in temperature is required.

During the four campaigns, carried out in various seasons the transmission behaviour was dominated by various phenomena and anomalies: strong refraction as well as haze conditions and high humidity.

7. ACKNOWLEDGEMENTS

All involved personnel from NRaD, now SPAWAR is greatly acknowledged for there support, especially Doug Jensen as great stimulator. Personnel from the BOQ at the Naval Subbase and the lifeguard station at Imperial Beach are greatly acknowledged for their help. At TNO-FEL Marco Roos, Hans Winkel and Ruud Kooijman are acknowledged for their technical support and data analysis.

The TNO participation in EOPACE is sponsored by the Netherlands MOD (assignment A95KM729) and the US Office of Naval Research ONR (grant N00014-96-1-0581).

8. REFERENCES

1. The IR and EO systems Handbook: Vol 2, SPIE Optical Engineering Press, 1993.
2. Session on MAPTIP at SPIE conference: Image propagation through the atmosphere, Denver, August 1996, SPIE Vol. 2828.
3. G. de Leeuw, 'Long-range IR propagation measurements over the North Sea', proceedings 55th AGARD-EPP specialists meeting, September 1994, Bremerhafen, Germany.
4. H.T. Bull, Near Surface Infrared Transmission Measurements, 1995, SPIE Vol. 2552, page 181-191.
5. Session on EOPACE at SPIE conference: Image propagation through the atmosphere, San Diego, July 1997, SPIE Vol. 3125.
6. A.N. de Jong, EOPACE Transmission Experiments Spring 1996, Preliminary Results, TNO report FEL-96-A090, March 1997.
7. A.N. de Jong, Transmission experiments during EOPACE, November 1996 and August/September 1997, Preliminary Results, TNO report FEL-97-A269, November1997.
8. A.N. de Jong, Long Range Transmission Measurements over Sea Water, report PHL 1978-08.
9. C. Zeisse, Low Elevation Transmission Measurements at EOPACE, Part I: Molecular and Aerosol effects, SPIE Vol. 3125-11.
10. A.N. de Jong, Low Elevation Transmission Measurements at EOPACE, Part III Scintillation Effects, SPIE Vol. 3125-13.
11. J.L. Forand, The L(W)WKD Marine Boundary Layer Model, Report DREV R-9618, March 1997, Unclassified.
12. D. Dion, On the analysis of atmospheric effects on EO sensors in the Marine Surface Layer, 2nd NATO-IRIS conference, London, June 1996.
13. S. Church, Atmospheric mirage and distortion modelling for IR target injection simulations, SPIE Vol. 2742, Orlando, April 1996.
14. W.H. Lehn, Analysis of an infrared mirage sequence, Applied Optics, Vol. 36, N° 21, July 1997.
15. A.T. Young, Sunset science, I The mock mirage, Applied Optics, Vol. 36, N° 12, April 1997.
16. W.D. Bruton, Unique temperature profiles for the atmosphere below an observer from sunset image, Applied Optics, Vol. 36, N° 27, September 1997.
17. M.E. Thomas, Astronomical refraction, Johns Hopkins APL Technical Digest, Volume 17, N° 3 (1996).
18. A.N. de Jong, Point target extinction and scintillation as function of range at LAPTEX, Crete, SPIE Vol. 3125-17, July 1997, San Diego.

RTO-MP-1
AC/323(SET)TP/2

RTO-MP-1

NORTH ATLANTIC TREATY ORGANIZATION

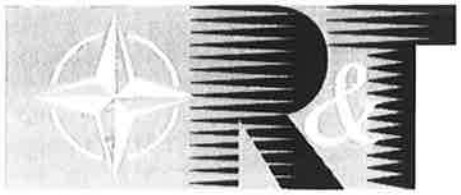

RESEARCH AND TECHNOLOGY ORGANIZATION
BP 25, 7 RUE ANCELLE, F-92201 NEUILLY-SUR-SEINE CEDEX, FRANCE

RTO MEETING PROCEEDINGS 1

E-O Propagation, Signature and System Performance Under Adverse Meteorological Conditions Considering Out-of-Area Operations

(La propagation, la signature et les performances des systèmes optroniques dans des conditions météorologiques défavorables, compte tenu des opérations hors zone)

Papers presented at the Sensors & Electronics Technology Panel Symposium held at the Italian Air Force Academy, Naples, Italy, 16-19 March 1998.

Published September 1998

Distribution and Availability on Back Cover